Asymmetrical 4-QAM for Totally Blind APP Channel Estimation

Marc C. Necker
Institute of Communication Networks and Computer Engineering,
University of Stuttgart
Pfaffenwaldring 47, D-70569 Stuttgart, Germany
Email: necker@ikr.uni-stuttgart.de
Tel.: +49 711 685 7963 Fax: +49711 685 7983

Frieder Sanzi
Institute of Telecommunications,
University of Stuttgart
Pfaffenwaldring 47, D-70569 Stuttgart, Germany
Email: sanzi@inue.uni-stuttgart.de
Tel.: +49 711 685 7941 Fax: +49 711 685 7929

***Abstract*— A new two-dimensional blind channel estimation scheme for coherent detection of OFDM signals in a mobile environment is presented. The channel estimation is based on the A Posteriori Probability (APP) calculation algorithm. The time-variant channel transfer function is completely recovered without phase ambiguity with no need for *any* pilot or reference symbols by using an asymmetrical 4-QAM signal point constellation. We study the impact of the constellation asymmetry on system performance by means of Extrinsic Information Transfer (EXIT) and BER charts. Our approach maximizes the spectral efficiency by avoiding any reference or pilot symbols and minimizes the BER by using coherent demodulation.**

I. Introduction

In wireless communication systems, channel estimation is a mandatory task for the receiver if coherent demodulation is used. In OFDM, channel estimation can conveniently be done by inserting a two-dimensional pattern of pilot symbols into the data stream. This allows the receiver to estimate the channel by means of FIR interpolation filters, such as Wiener-filters [1]. This concept was successfully applied in Digital Video Broadcasting – Terrestrial (DVB-T) [2], for example. As an alternative, differentially coherent demodulation can be used. This, however, leads to a loss in E_b/N_0 of approximately $2\,\mathrm{dB}$ for AWGN channels and larger losses for fading channels [3].

Channel estimation based on Wiener-filters requires a minimum number of pilot symbols depending on the worst case channel conditions [1]. In DVB-T, this overhead is more than 10%. Instead of using FIR filters, the authors of [4] developed a channel estimation algorithm based on the calculation of the A Posteriori Probability (APP). The two-dimensional channel transfer function (CTF) is estimated by concatenating two one-dimensional APP estimators in frequency and time direction, respectively. This method dramatically reduces the amount of pilot symbols compared to FIR interpolation. Furthermore, the APP channel estimator can be embedded in an iterative decoding loop with a soft in/soft out decoder.

Beyond that, a better spectral efficiency can be achieved by using blind channel estimation algorithms, which make pilot symbols unnecessary. Most blind estimation algorithms are based on higher order statistics and converge slowly, making them unsuitable for mobile environments. Examples include those using correlation methods [5] and cumulant fitting schemes [6]. Other blind channel estimation algorithms for OFDM take advantage of the redundancy which is introduced by the cyclic prefix [7].

In any case, a phase ambiguity is introduced in the channel estimate, which makes at least one reference symbol necessary to resolve. In [8] the authors present a fast converging totally blind channel estimator based on the Maximum Likelihood principle, which recovers the amplitude and phase of a channel without the need for any reference symbols by combining modulation schemes, such as QPSK and 3-PSK.

In this paper we combine the idea of totally blind [8] and APP channel estimation (APP-CE) [4]. We use modulation schemes with an asymmetrical arrangement to solve the phase ambiguity problem. The performance is evaluated with a fast-varying mobile channel on the basis of Extrinsic Information Transfer (EXIT) [9] and BER charts.

Our paper is structured as follows: An overview of the system model is given in section II. Section III introduces the totally blind channel estimation algorithm. Finally, section IV evaluates the performance of the presented system.

II. System Model

A. Transmitter and Receiver

We investigate an OFDM-system with $K = 1001$ subcarriers having a carrier-spacing of $\Delta f = 4\,\mathrm{kHz}$ and an OFDM-symbol duration (useful part plus guard interval) of $T_\mathrm{s} = 312.5\,\mu\mathrm{s}$. We combine $L = 100$ successive OFDM symbols for a blockwise transmission. The signal from the binary source is convolutionally encoded and interleaved as shown in Fig. 1. After interleaving, 2 successive coded bits are grouped and mapped onto a 4-QAM symbol $X_{k,l}$ with asymmetrical arrangement as shown in Fig. 2. We use Gray-Mapping throughout the paper. The signal $X_{k,l}$ is modulated onto K orthogonal subcarriers by an iFFT-block. Finally, a cyclic prefix of length 1/4 is inserted.

We obtain the received 4-QAM signal constellation points $Y_{k,l}$ by removing the cyclic prefix and OFDM demodulation:

$$Y_{k,l} = H_{k,l} \cdot X_{k,l} + N_{k,l}, \tag{1}$$

where l is the OFDM symbol index, k is the subcarrier index and $N_{k,l}$ are statistically i.i.d. complex Gaussian noise variables with component-wise noise power $\sigma_N^2 = N_0/2$. The $H_{k,l}$ are sample values of the CTF:

$$H_{k,l} = H(k \cdot \Delta f, l \cdot T_\mathrm{s}) \tag{2}$$

At the receiver, an iterative APP-CE is applied [4]. The

International OFDM-Workshop (InOWo), Hamburg, Germany, September 2003, pp. 75-79.

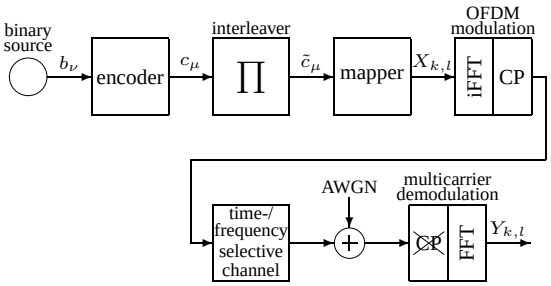

Fig. 1: Transmitter and channel model.

signal $Y_{k,l}$ is fed to the blind APP-CE stage as shown in Fig. 3. This stage outputs log-likelihood ratios (L-values) on the transmitted coded bits which are deinterleaved and decoded in an APP decoder. Iterative channel estimation and decoding is performed by feeding back extrinsic information on the coded bits; after interleaving it becomes the *a-priori* knowledge to the blind APP-CE stage. The APP-CE stage is explained in more detail in section III-B.

We use a recursive systematic convolutional code with feedback polynomial $G_\mathrm{r} = 037_8$, feed-forward polynomial $G = 023_8$, memory 4 and code rate $R_\mathrm{c} = 0.5$. Note that in the following all E_b/N_0-values are given with respect to the overall information rate $R = R_\mathrm{c} \cdot R_\mathrm{g} = 0.4$, whereby R_g considers the redundancy introduced by the cyclic prefix:

$$R_\mathrm{g} = \frac{1}{\Delta f \cdot T_\mathrm{s}} = 0.8 \tag{3}$$

B. Channel Model

For the performance evaluation we assumed a frequency-selective fading channel according to a wide-sense stationary uncorrelated scattering (WSSUS) model. The channel was simulated according to the model introduced in [10], which describes the channel's time-variant impulse response as

$$h(\tau,t) = \lim_{Z\to\infty} \frac{1}{\sqrt{Z}} \sum_{m=1}^{Z} e^{j\theta_m} e^{j2\pi f_{\mathrm{D}max} t} \delta(\tau - \tau_{max}) \,. \tag{4}$$

The Fourier-Transform of equation (4) with respect to τ yields the channel's time-variant frequency response:

$$H(f,t) = \lim_{Z\to\infty} \frac{1}{\sqrt{Z}} \sum_{m=1}^{Z} e^{j\theta_m} e^{j2\pi f_{\mathrm{D}max} t} e^{-j2\pi f \tau_{max}} \,. \tag{5}$$

For each of the Z paths, the phase-shift θ_m, the Doppler-shift $f_{\mathrm{D}_{max}}$ and the delay τ_m are randomly chosen from the corresponding probability density function (pdf) $p_\theta(\theta)$, $p_{f_\mathrm{D}}(f_\mathrm{D})$

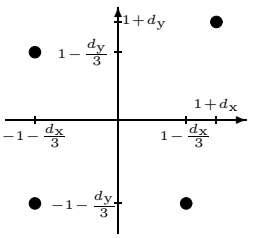

Fig. 2: 4-QAM constellation diagram with asymmetrical arrangement.

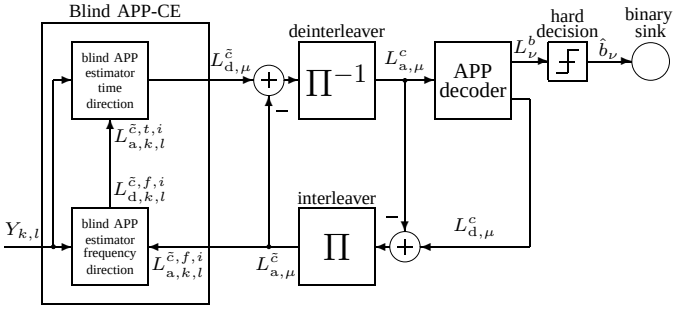

Fig. 3: Receiver with iterative blind APP channel estimation.

or $p_\tau(\tau)$ of the channel model [10]. For the simulations, the number of paths was chosen to be $Z = 100$.

In our model, the phase θ is uniformly distributed between 0 and 2π. For the delay τ we assume an exponentially decaying pdf $p_\tau(\tau)$ with τ_max being the channel delay spread chosen such that $p_\tau(\tau_\mathrm{max})/p_\tau(0) = 1/1000$. The pdf of the Doppler frequency $p_{f_\mathrm{D}}(f_\mathrm{D})$ is assumed to be of Jakes' type whereby $f_{\mathrm{D}_\mathrm{max}}$ denotes the maximal Doppler shift.

With these assumptions the complex auto-correlation function of $H(f,t)$ in frequency direction is given by

$$R_{f;\Delta k} = \frac{1 - e^{-\tau_\mathrm{max}(\frac{1}{\tau_\mathrm{rms}} + j2\pi\cdot\Delta k\cdot\Delta f)}}{(1 - e^{-\frac{\tau_\mathrm{max}}{\tau_\mathrm{rms}}}) \cdot (1 + j2\pi\cdot\Delta k\cdot\Delta f\cdot\tau_\mathrm{rms})} \,, \tag{6}$$

whereby Δk is the difference of two discrete frequency indexes. For the auto-correlation function of $H(f,t)$ with respect to t we obtain

$$R_{t;\Delta l} = J_0(2\pi f_{\mathrm{D}_\mathrm{max}} \cdot \Delta l \cdot T_\mathrm{s}) \,. \tag{7}$$

Δl is the difference of two discrete time indexes. J_0 is the Bessel function of zero order. The expected value yields to

$$\mathrm{E}\left\{H_{k,l} \cdot H^*_{k',l'}\right\} = R_{f;(k-k')} \cdot R_{t;(l-l')} \,, \tag{8}$$

whereby * denotes the conjugate complex operation. Please refer to [10] and [11] for the derivation of (6) – (8).

III. Totally Blind APP Channel Estimation

A. Totally blind Channel Estimation

The totally blind channel estimation algorithm in [8] is based on the Maximum Likelihood (ML) principle as presented in [12]. One of the key problems is the following maximization equation, which needs to be solved:

$$\hat{\Psi} = \min_{\Psi} \|\mathbf{y} - \mathbf{X}\mathbf{A}_d\mathbf{h}\|^2 \quad , \quad \Psi := [\mathbf{h}^T, \mathbf{x}^T]^T \,. \tag{9}$$

$\mathbf{h}$ is a length-G vector of taps of the discrete-time channel impulse response. $\mathbf{x}$ and $\mathbf{y}$ are vectors with M symbols transmitted and received on adjacent subcarriers, respectively. $\mathbf{X}$ is a diagonal matrix containing the corresponding transmitted data symbols as diagonal elements. $\mathbf{A}_d$ is the DFT matrix:

$$\begin{aligned} \mathbf{A}_d &= [\mathbf{a}_{d,0}\ \mathbf{a}_{d,1}\ \cdots\ \mathbf{a}_{d,G-1}] \,, \\ \mathbf{a}_{d,m} &= [1\ \ e^{-jm\Delta\omega T_s}\ \ \cdots\ \ e^{-jm\Delta\omega T_s(M-1)}]^T \end{aligned} \,, \tag{10}$$

with $\Delta\omega$ being the subcarrier spacing $\Delta\omega = 2\pi/KT_s$.

In [12], the authors used a branch-and-bound integer programming strategy to solve the maximum equation (9). In [8], the autocorrelation of the CTF in frequency direction was taken advantage of in order to reduce the number of elements in the vectors and matrices of (9). It was shown that as few as two data symbols on adjacent subcarriers are sufficient to estimate the channel transfer function, which makes it trivial to solve (9). A suboptimal approach was presented which significantly reduces the complexity of the optimization problem when more than two subcarriers are considered.

One of the main contributions of [8] was the resolution of the channel estimate's phase ambiguity without using any reference symbols, even in fast varying mobile environments. This was achieved by using two different PSK-modulation schemes on adjacent subcarriers. Let q_i be a signal point of the first modulation scheme and q_j a signal point of the second scheme. If $\alpha_{i,j} = \angle(q_i, q_j)$ denotes the angle between both signal points in the complex plane, the signal points of the modulation schemes must be chosen such that no two angles $\alpha_{i,j}$ are identical for all possible signal point combinations i, j. For example, QPSK and 3-PSK fulfill this condition.

If the CTF does not vary fast in frequency direction (i.e. the autocorrelation meets certain conditions), the receiver can determine the symbols $X_{k,l}$ and $X_{k+1,l}$ sent on adjacent subcarriers unambiguously [8]. Simulations showed that this concept delivers good BER-performance with COST207-channels RA and TU. For channels with longer delay spreads, this concept imposes problems as the condition of a slowly varying CTF in frequency direction only holds for some subcarriers.

B. Iterative totally blind APP Channel Estimation

The two-dimensional blind APP channel estimator consists of one estimator for frequency and time direction, respectively [4]. The estimation algorithm exploits the time and frequency continuity of the CTF at the receiver. It calculates the most likely sent symbol sequence conditioned on the received symbol sequence with respect to the channel's autocorrelation functions. If symmetrical modulation schemes are used, the transmission of pilot symbols is mandatory [4]. Without pilots, every symbol sequence $e^{j\varphi}X_{k,l}$, $\varphi = 0$, $\frac{1}{2}\pi$, π, $\frac{3}{2}\pi$, would be a possible solution to the APP estimator. If we use a combination of modulation schemes as described above, this ambiguity vanishes. Moreover, since the APP estimator considers very large blocks with sizes of $L \cdot K$ symbols, we get along by using only one asymmetrical modulation scheme, such as the 4-QAM scheme of Fig. 2. If we assume a uniform distribution of transmitted signal points[1], there is only one phase φ with $e^{j\varphi}X_{k,l}$ which delivers a solution in the APP estimator due to the asymmetry of the data symbols.

For one-dimensional APP estimation, the symbol-by-symbol MAP-algorithm is applied to an appropriately chosen metric. To help understanding, the symbols $X_{k,l}$ at the transmitter in Fig. 1 can be thought of being put into a virtual shift register at the output of the mapper. Owing to this "artificial grouping" the corresponding trellis exploits the time and frequency continuity of the CTF at the receiver.

[1]This is reasonable due to the application of error correction codes

At frequency index k, the APP estimation in frequency direction is characterized for OFDM symbol l_0 with $0 \le l_0 \le L-1$ by the metric increment

$$\gamma_k = -\frac{|Y_{k,l_0} - \hat{H}^f_{k,l_0} \cdot \hat{X}_{k,l_0}|^2}{2 \cdot \sigma_f^2} + \sum_{i=0}^{1} d^i_{k,l_0} \cdot L^{\tilde{c},f,i}_{\mathrm{a},k,l_0} \qquad (11)$$

with estimated channel coefficient

$$\hat{H}^f_{k,l_0} = \sum_{i=1}^{m_f} u_{f,i} \cdot \frac{Y_{k-i,l_0}}{\hat{X}_{k-i,l_0}} \; . \qquad (12)$$

The $\hat{X}_{k,l_0}$ denote the hypothesized transmitted data symbol according to the trellis structure. The $L^{\tilde{c},f,i}_{\mathrm{a},k,l_0}$ in (11) are the *a-priori* L-values of the coded bits $\tilde{c}_\mu$ which are fed to the APP estimator in frequency direction. The bits d^0_{k,l_0} and d^1_{k,l_0} in the sum in (11) result from the hard demapping of $\hat{X}_{k,l_0}$. The calculation of the prediction coefficients $u_{f,i}$ in (12) and the derivation of the variance $2 \cdot \sigma_f^2$ of the error in (11) are described in section III-C. m_f is the prediction order in frequency-direction.

Accordingly, at time index l, the APP estimation in time direction is characterized for subcarrier k_0 with $0 \le k_0 \le K-1$ by the metric increment

$$\gamma_l = -\frac{|Y_{k_0,l} - \hat{H}^t_{k_0,l} \cdot \hat{X}_{k_0,l}|^2}{2 \cdot \sigma_t^2} + \sum_{i=0}^{1} d^i_{k_0,l} \cdot L^{\tilde{c},t,i}_{\mathrm{a},k_0,l} \qquad (13)$$

with estimated channel coefficient

$$\hat{H}^t_{k_0,l} = \sum_{i=1}^{m_t} u_{t,i} \cdot \frac{Y_{k_0,l-i}}{\hat{X}_{k_0,l-i}} \; . \qquad (14)$$

m_t is the prediction order in time-direction. The two 1D APP estimators are concatenated as shown in Fig. 3. The output $L^{\tilde{c},f,i}_{\mathrm{d},k,l}$ of the APP estimator in frequency direction becomes the *a-priori* input $L^{\tilde{c},t,i}_{\mathrm{a},k,l}$ of the APP estimator in time direction.

C. Linear Prediction Coefficients

The approach to obtain the linear prediction coefficients in frequency (12) and time (14) is similar. Therefore, we restrict our derivation to the coefficients in frequency direction.

For the calculation of the linear prediction coefficients $u_{f,i}$ we assume, that the current state in the trellis actually was transmitted. Under this assumption, (12) can be expressed as

$$\hat{H}^f_{k,l_0} = \sum_{i=1}^{m_f} u_{f,i} \cdot \hat{H}_{k-i,l_0} \; , \qquad (15)$$

whereby

$$\hat{H}_{k-i,l_0} = H_{k-i,l_0} + \frac{N_{k-i,l_0}}{\hat{X}_{k-i,l_0}} \; . \qquad (16)$$

Taking (8) and (16) into account, we can compute the expected value

$$\mathrm{E}\left\{\hat{H}_{k-i,l_0} \cdot \hat{H}^*_{k-\tilde{i},l_0}\right\} = R_{f;\tilde{i}-i} + \delta_{\tilde{i}-i} \cdot \frac{N_0}{\left|\hat{X}_{k-i,l_0}\right|^2} \qquad (17)$$

and the expected value

$$\mathrm{E}\left\{H_{k,l_0}\cdot\hat{H}^{*}_{k-i,l_0}\right\}=R_{f;i}\ . \tag{18}$$

We calculate the linear prediction coefficients solving the Wiener-Hopf equation in order to minimize the mean squared error $\mathrm{E}\left\{\left|H_{k,l_0}-\hat{H}^{f}_{k,l_0}\right|^2\right\}$. Therefore, the linear prediction coefficients are:

$$\left(u_{f,1},\ldots,u_{f,m_f}\right)=\mathbf{r}_f^T\cdot\mathbf{R}_f^{-1} \tag{19}$$

Taking (18) into account, the vector $\mathbf{r}_f^T$ can be calculated as:

$$\mathbf{r}_f^T=\left(R_{f,1},\ldots,R_{f,m_f}\right) \tag{20}$$

Using (17), we obtain the matrix $\mathbf{R}_f$ as:

$$\mathbf{R}_f=\begin{pmatrix} 1+\frac{N_0}{\hat{X}_{k-1,l_0}} & R_{f,1} & \cdots & R_{f,m_f-1}\\ R_{f,-1} & 1+\frac{N_0}{\hat{X}_{k-2,l_0}} & & R_{f,m_f-2}\\ \vdots & & \ddots & \vdots\\ R_{f,-m_f+1} & \cdots & R_{f,-1} & 1+\frac{N_0}{\hat{X}_{k-m_f,l_0}} \end{pmatrix} \tag{21}$$

The minimum mean squared error results to:

$$J_{\min,f}=1-\mathbf{r}_f^T\cdot\mathbf{R}_f^{-1}\cdot\mathbf{r}_f^{*} \tag{22}$$

Therefore, the term $2\cdot\sigma_f^2$ in (11) yields to:

$$2\cdot\sigma_f^2=N_0+J_{\min,f}\cdot\left|\hat{X}_{k,l_0}\right|^2 \tag{23}$$

Note that the absolute value of the 4-QAM signal points in Fig. 2 is not constant. This is taken into account by using the absolute value $|\hat{X}_{k-i,l_0}|$ of a hypothesized symbol in (17). As a consequence, each state in the trellis has its own linear prediction coefficients and minimum mean squared error. Beyond, each branch in the trellis has its own variance $2\cdot\sigma_f^2$ of the error, which directly results from (23).

IV. Simulation results

We first investigate the influence of the parameters d_x and d_y on the system performance. Fig. 4 shows the EXIT charts for $f_{\mathrm{D}_{\max}}=300\,\mathrm{Hz}$, $\tau_{\max}=40\,\mu\mathrm{s}$ and four different values of $d_x=d_y$. The EXIT charts show the characteristic curve of the blind APP-CE stage at $E_\mathrm{b}/N_0=8\,\mathrm{dB}$ and the characteristic curve of the convolutional decoder. The trajectories in the diagrams show the information exchange between these two stages. For $d_x=d_y=0.05$, the two characteristic curves intersect at $\mathrm{I_{E2}}\approx 0$, which is why no trajectory is visible. Consequently, the BER is on the order of 50%. As $d_x=d_y$ are increased, the starting point of the APP-CE's characteristic curve at $\mathrm{I_{E2}}=0$ moves towards higher mutual information values $\mathrm{I_{E1}}$. Yet, the intersection point with the decoder's characteristic curve is the same for all considered $d_x=d_y\geq 0.15$. As a consequence, we can compensate for the lower starting point with more iterations.

Looking at $d_x=d_y=0.05$ in detail, Fig. 5 depicts the EXIT charts for higher values of $E_\mathrm{b}/N_0=11\,\mathrm{dB}$ and $12\,\mathrm{dB}$. It is most important to notice that the starting point of the

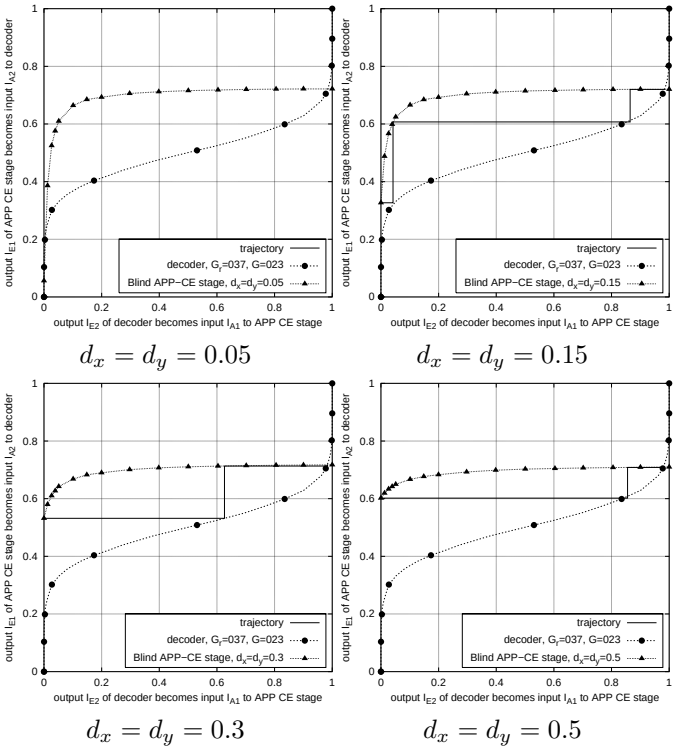

$d_x=d_y=0.05$ $\quad$ $d_x=d_y=0.15$

$d_x=d_y=0.3$ $\quad$ $d_x=d_y=0.5$

Fig. 4: EXIT chart, blind APP-CE stage and decoder with simulated trajectory of the iterative decoding loop at $E_\mathrm{b}/N_0=8\,\mathrm{dB}$. $f_{\mathrm{D}_{\max}}=300\,\mathrm{Hz}$ and $\tau_{\max}=40\,\mu\mathrm{s}$.

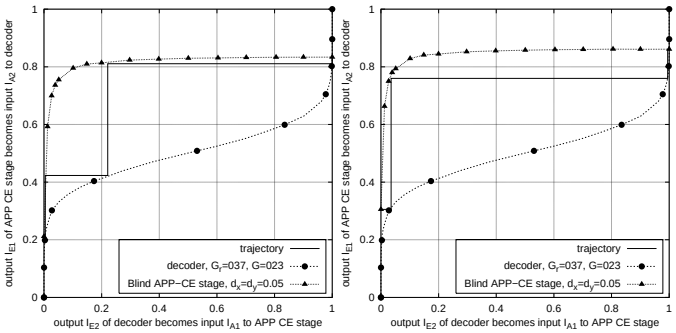

$E_\mathrm{b}/N_0=11\,\mathrm{dB}$ $\quad$ $E_\mathrm{b}/N_0=12\,\mathrm{dB}$

Fig. 5: EXIT chart, blind APP-CE stage and decoder with simulated trajectory of the iterative decoding loop for $d_x=d_y=0.05$. $f_{\mathrm{D}_{\max}}=300\,\mathrm{Hz}$ and $\tau_{\max}=40\,\mu\mathrm{s}$.

channel estimator's trajectory moves to higher values $\mathrm{I_{E1}}$. For $E_\mathrm{b}/N_0=12\,\mathrm{dB}$, there is a good gap between the two characteristic curves at $\mathrm{I_{E2}}\approx 0$. This gap becomes very small for $E_\mathrm{b}/N_0=11\,\mathrm{dB}$. Consequently, the trajectory will not be able to escape depending on the condition of the time-varying mobile channel, leading to a degradation in BER performance.

The EXIT charts reflect itself in the BER chart of Fig. 6, which shows the BER for various positive and negative values of $d_x=d_y$. As can be seen, the BER performance of a negative $d_x=d_y$ is slightly better than the BER performance of the corresponding positive value. At a high E_b/N_0, all curves are virtually identical. This is supported by the EXIT charts,

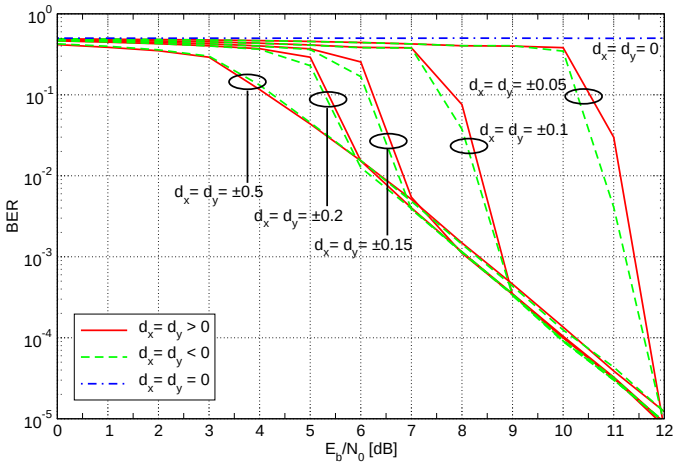

Fig. 6: BER after 4 iterations for various positive and negative values of d_x and d_y. $f_{\mathrm{D_{max}}} = 300\,\mathrm{Hz}$ and $\tau_{\mathrm{max}} = 40\,\mu\mathrm{s}$.

since the point of intersection of the characteristic curves is the same for all considered $d_x = d_y$. Finally, for a target BER of 10^{-4}, an asymmetry of $d_x = d_y = \pm 0.1$ is sufficient.

If we investigate a more moderate channel, the performance of the system improves significantly. Fig. 7 shows the BER performance for $f_{\mathrm{D_{max}}} = 100\,\mathrm{Hz}$, $\tau_{\mathrm{max}} = 20\,\mu\mathrm{s}$ and several values of $d_x = d_y$. The general characteristics are the same as in Fig. 6. However, for a target BER of 10^{-3}, a smaller asymmetry of $d_x = d_y = -0.05$ is sufficient. For $d_x = d_y = \pm 0.1$, the BER is already excellent in desirable BER ranges. Hence, by choosing $d_x = d_y = \pm 0.1$, a good BER performance can be achieved over a wide range of channel parameters.

The influence of the iteration loop can be seen in Fig. 8. The chart shows the BER performance for $f_{\mathrm{D_{max}}} = 300\,\mathrm{Hz}$, $\tau_{\mathrm{max}} = 40\,\mu\mathrm{s}$ and $d_x = d_y = 0.15$ after different number of iterations. The iterative behavior of the system follows exactly the trajectory of the corresponding EXIT chart in Fig. 4. Depending on the required BER, only two iterations are sufficient.

V. Conclusion

We combined the concept of totally blind channel estimation based on combined modulation schemes, and the idea of APP channel estimation. The result is a channel estimator, that is capable of estimating the channel transfer function without the need for any pilot or reference symbols even in a rapidly time-varying mobile environment. Our results clearly indicate that blind channel estimation is possible for virtually any realistic time-variant mobile channel.

References

[1] P. Höher, S. Kaiser, and P. Robertson, "Two–dimensional pilot–symbol–aided channel estimation by Wiener filtering," in *ICASSP*, Munich, Germany, April, 1997, pp. 1845–1848.

[2] "Digital video broadcasting (DVB); framing structure, channel coding and modulation for digital terrestrial television (DVB-T)," *European Telecommunication Standard, ETS 300744*, March 1997.

[3] J. G. Proakis, *Digital Communications*. McGraw-Hill, 1995.

[4] F. Sanzi and S. ten Brink, "Iterative channel estimation and decoding with product codes in multicarrier systems," in *Proc. IEEE Vehicular Tech. Conf. (VTC–Fall)*, Boston, USA, September, 2000, pp. 1338–1344.

[5] B. Muquet and M. de Courville, "Blind and semi-blind channel identification methods using second order statistics for OFDM systems," in *Proc. IEEE ICASSP*, Phoenix, AZ, USA, March, 1999, pp. 2745–2748.

[6] S. Chen, Y. Wu, and S. McLaughlin, "Genetic algorithm optimization for blind channel identification with higher order cumulant fitting," vol. 1, no. 4, pp. 259–265, November, 1997.

[7] U. Tureli and H. Liu, "Blind carrier synchronization and channel identification for OFDM communications," in *Proc. IEEE ICASSP*, Seattle, WA, USA, May, 1998, pp. 3509–3512.

[8] M. Necker and G. Stüber, "Totally blind channel estimation for OFDM over fast varying mobile channels," in *Proc. IEEE Intern. Conf. on Comm.*, New York, USA, April, 2002, pp. 421–425.

[9] S. ten Brink, "Convergence behavior of iteratively decoded parallel concatenated codes," *IEEE Trans. on Comm.*, vol. 49, no. 10, pp. 1727–1737, October, 2001.

[10] P. Höher, "A statistical discrete-time model for the WSSUS multipath channel," *IEEE Trans. on Veh. Tech.*, vol. 41, no. 4, pp. 461–468, November, 1992.

[11] F. Sanzi, S. Jelting, and J. Speidel, "A comparative study of iterative channel estimators for mobile OFDM systems," *IEEE Trans. on Wireless Comm.*, vol. 2, no. 5, September, 2003.

[12] N. Chotikakamthorn and H. Suzuki, "On identifiability of OFDM blind channel estimation," in *Proc. Vehicular Technology Conference 1999 - Fall*, Amsterdam, The Netherlands, September 1999, pp. 2358–2361.

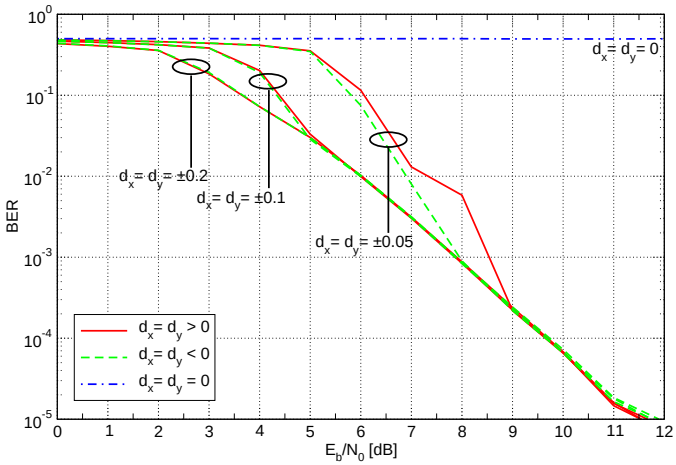

Fig. 7: BER after 4 iterations for various positive and negative values of d_x and d_y. $f_{\mathrm{D_{max}}} = 100\,\mathrm{Hz}$ and $\tau_{\mathrm{max}} = 20\,\mu\mathrm{s}$

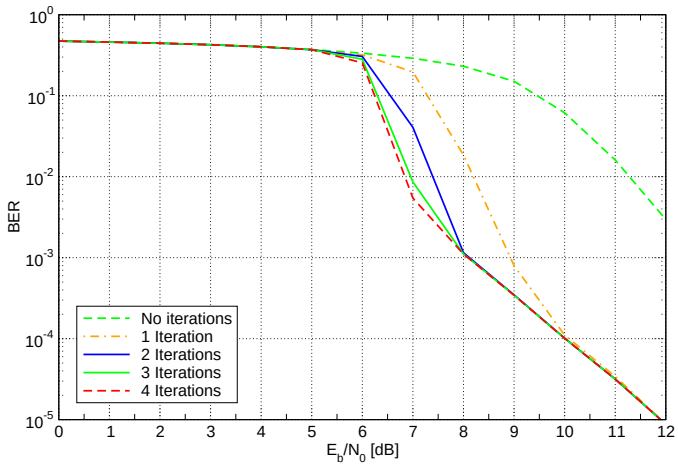

Fig. 8: BER for $d_x = d_y = 0.15$ after different numbers of iterations. $f_{\mathrm{D_{max}}} = 300\,\mathrm{Hz}$ and $\tau_{\mathrm{max}} = 40\,\mu\mathrm{s}$